Availability-Aware Service Provisioning in EONs: How Efficient will FIPP-*p*-Cycles be?

Shilin Zhu[1], Siyao Meng[1], Qinkun Bao[1], Xiaoliang Chen[1], Zuqing Zhu[1]

1. University of Science and Technology of China, Hefei, Anhui 230027, China, Email: zqzhu@ieee.org

Abstract: We propose to realize availability-aware service provisioning in EONs with FIPP-*p*-cycles and bandwidth-squeezed restoration. Simulation results show that the proposed schemes are more reliable and spectrum-efficient than the existing approach.

OCIS codes: (060.4261) Networks, protection and restoration; (060.4257) Networks, network survivability.

1. Introduction

Elastic optical networks (EONs) achieve flexible spectrum allocation by setting up lightpaths with series of narrow-band and spectrally-contiguous frequency slots (FS'). Meanwhile, network survivability and service recoverability are vital in optical networks since a single fiber-cut can cause tremendous data loss. Previously, people have designed both path- and link-based schemes to protect EONs against single-link failures [1, 2]. Moreover, it is known that by considering service availability, which is defined as the ratio of service-on time to the total provisioning period, network operators can use availability-aware service provisioning (AaSP) to achieve efficient and differentiated protection for clients with various service-level agreements (SLAs) [3]. Note that, with the flexible spectrum allocation, the AaSP in EONs will be more efficient and sophisticated than that in traditional wavelength-division multiplexing (WDM) networks, especially when bandwidth-squeezed restoration is applied [4]. In this paper, we study how to leverage failure-independent path-protecting pre-configured cycles (FIPP-*p*-cycles) [5, 6] to achieve spectrum-efficient AaSP in EONs. We first incorporate bandwidth-squeezed restoration to design a novel AaSP scheme using FIPP-*p*-cycles and analyze the service availability for this scheme theoretically to assist the design. Then, we propose a topology-partition based protection strategy to reduce the time complexity of the proposed algorithm. Numerical simulations indicate that compared with the existing approach in literature, our proposed algorithms can achieve ∼**50%** spectrum-saving.

2. Bandwidth-Squeezed AaSP with FIPP-*p*-Cycles (AaSP-FIPP)

We model the EON topology as $G(V,E)$, where V and E are the sets of nodes and fiber links, respectively. The lightpath request can be modeled as $LR(s,d,B,A)$, where s and d are source and destination, B is bandwidth requirement in number of FS', and A is availability requirement. Basically, the service of a request is on, if its working path is available or it secures the backup resources successfully when the working path is broken. Note that, with bandwidth-squeezed restoration, EONs can use a restoration bandwidth B' that is less than B to recover the request's service partially [4]. Hence, we can assume that the acquired availability during the bandwidth-squeezed restoration is also proportional to B', as $A' = \frac{B'}{B}$. Meanwhile, we should notice that B' cannot be arbitrarily small as each request should have a minimum and un-squeezable bandwidth requirement B_m for non-disrupted service [4]. Hence, we have $A' = 0$ when $B' < B_m$. For example, if a request has $B = 10$ FS' and $B_m = 7$ FS', its acquired availability $A' = 0.8$ if it is allocated 8 FS' during restoration. Otherwise, if 7 or more FS' cannot be allocated, we consider its service as disrupted with $A' = 0$.

For a request $LR(s,d,B,A)$, the bandwidth-squeezed AaSP with FIPP-*p*-cycles (AaSP-FIPP) first performs routing and spectrum allocation (RSA) to set up the working path. If its availability requirement can be satisfied with only a working path, AaSP-FIPP just provisions LR as unprotected. Otherwise, AaSP-FIPP either builds an FIPP-*p*-cycle to protect it or makes it to share an existing FIPP-*p*-cycle with other in-service requests. In both cases, the working path of LR has its two end-nodes on the FIPP-*p*-cycle, while its protection path is on the FIPP-*p*-cycle. We also have spectra pre-allocated to the FIPP-*p*-cycle to reduce the switch reconfiguration latency during restoration. Here, to improve spectrum-efficiency, we can use the bandwidth-squeezed restoration for LR as long as its availability requirement is satisfied. This means that LR only obtains a restoration bandwidth $B' < B$ on the FIPP-*p*-cycle, even if it is the only affected request due to link-failure(s). Hence, we define an initial bandwidth-squeezing ratio of LR as $\gamma_0 = \frac{B'}{B}$.

As AaSP-FIPP determines the protection scheme of LR based on its availability requirement, we then perform theoretical analysis to obtain the availability expressions for unprotected and FIPP-*p*-cycle schemes. If we assume that the hop-count of the working path is H_w, the availability of the unprotected scheme is $A_L = \rho^{Hw}$, where ρ is the link availability, *i.e.*, assumed as identical for each link in the EON. While for the FIPP-*p*-cycle scheme, the availability is

$$A_L = \rho^{Hw}\left\{1 + H_w(1-\rho)\rho^{H_p-1}\left[\rho^{|\mathbf{L}|}\gamma_0 + \sum_{e\in\mathbf{L}}\rho^{|\mathbf{L}|-1}(1-\rho)(\frac{1}{2}\gamma_0 + \frac{1}{2}\gamma_e) + \frac{1}{2}(H_w-1)(1-\rho)\rho^{|\mathbf{L}|-1}\gamma_0\right]\right\}. \quad (1)$$

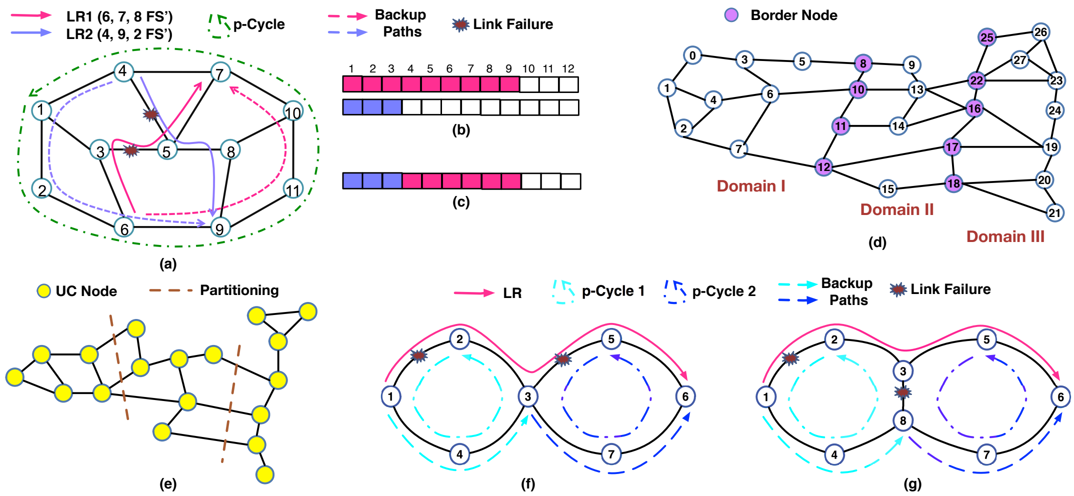

Fig. 1. (a) EON with FIPP-*p*-cycle, (b) FS' allocated for working paths, (c) FS' used for backup paths during restoration, (d) US Backbone topology, (e) Auxiliary graph, (f) Normal inter-domain failures, (g) Special inter-domain failures.

Here, we define $\mathbf{L}$ as the set of links on the working paths of the in-service requests that share backup FS' with LR, H_p is the hop-count of LR's backup path on the FIPP-p-cycle, and γ_e is the acquired bandwidth-squeezing ratio to tell us how many backup FS' LR can get on the FIPP-p-cycle if link e has already been broken. Note that, $\gamma_e = 0$ if the acquired backup FS' are less than B_m. Figs. 1(a) and 1(b) show an example of AaSP-FIPP. Here, $LR_1(Node\ 6, Node\ 7, 8\ FS')$ shares the backup FS' with $LR_2(Node\ 4, Node\ 9, 2\ FS')$ on an FIPP-p-cycle, and we reserve 9 FS' (*i.e.*, with one guard-band FS) to protect them. Hence, for both LR_1 and LR_2, we have $\gamma_0 = 1$. We then consider two link-failures on *Links* 4-5 and 3-5 in sequence. When *Link* 4-5 fails, LR_2 can be fully restored as it can get 3 FS' (*i.e.*, with one guard-band FS) on its protection path. Then, the failure on *Link* 3-5 makes LR_1 switch to its protection path. As there are only 6 pre-allocated FS' left on *Link* 6-9, LR_1 uses the bandwidth-squeezed restoration in Fig. 1(c), with $\gamma_e = \frac{5}{8}$.

3. Bandwidth-Squeezed AaSP with Topology-Partitioned FIPP-*p*-Cycles (AaSP-TP-FIPP)

As AaSP-FIPP needs to check the cycles in the network topology to set up the FIPP-p-cycles and to achieve the sharing of backup FS', its time complexity can increase quickly with the scale of the topology. In order to control the time complexity, we develop a topology-partitioned scheme (AaSP-TP-FIPP) to divide the EON into a few domains and apply AaSP-FIPP to each domain. For the request that traverses multiple domains, the FIPP-p-cycle in each domain can protect it. For example, in Fig. 1(f), we use two FIPP-p-cycles to protect a request.

For AaSP-TP-FIPP, we can analyze the service availability of an LR by considering the intra-domain and inter-domain cases. Apparently, the intra-domain availability can be obtained with the expressions in Section 2. While for the inter-domain case, we generally have two scenarios when the link-failures happen in different domains, as shown in Figs. 1(f) and 1(g). Note that, in an optical network, the link availability usually approaches to 1, which means that the probability of concurrent link-failures is very low, and thus we only consider dual link-failures here, same as that in [5]. In Fig. 1(f), both link-failures happen on the working path, the protection paths can be established on the two FIPP-p-Cycles. For the case in Fig. 1(g), when a failure happens on the edge-link in between two domains, *Node* 8 detects the failure and triggers the path switching. Then, the inter-domain service availability of LR is

$$A_{inter} = (1-\rho)^2 \rho^{\left(\sum_{k=1}^{|\mathbf{D}|}|\mathbf{L}_k^w|\right)} \left\{ \sum_{e_1\in \mathbf{L}_i^w}\ \sum_{e_2\in\mathbf{L}_j^w, j\neq i} \rho^{\left(|\mathbf{L}_i^p|+|\mathbf{L}_j^p|-|\mathbf{L}_i^w|-|\mathbf{L}_j^w|\right)} + \sum_{e_1\in\mathbf{L}_i^w}\ \sum_{e_2\in(\mathbf{L}_i^p\bigcap\mathbf{L}_j^p)} \rho^{\left(|\mathbf{L}_i^{p,*}|+|\mathbf{L}_j^{p,*}|-|\mathbf{L}_i^w|-|\mathbf{L}_j^w|\right)} \right\}, \quad (2)$$

where $\mathbf{D}$ represents the set of domains from topology partition, $\mathbf{L}_i^w$ is the set of links on the working path of LR in domain $D_i \in \mathbf{D}$, $\mathbf{L}_i^p$ is the set of links on the protection path of LR in domain D_i, and $\mathbf{L}_i^{p,*}$ is the set of links on the revised protection path of LR in domain D_i when a failure happens on the edge links (*e.g.*, the special case in Fig. 1(g)). Finally, the overall service availability of LR should be

$$A_L = \rho^{\left(\sum_{i=1}^{|\mathbf{D}|}|\mathbf{L}_i^w|\right)} + \sum_{i=1}^{|\mathbf{D}|}\left[(A_{L,i}-\rho^{|\mathbf{L}_i^w|})\rho^{\left(\sum_{j=1}^{|\mathbf{D}|}|\mathbf{L}_j^w|-|\mathbf{L}_i^w|\right)}\right] + A_{inter}, \quad (3)$$

where $A_{L,i}$ is the intra-domain availability in domain D_i calculated with expressions in Section 2.

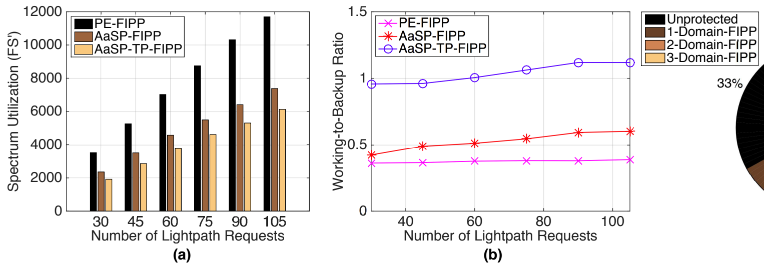

RESULTS ON RUNNING TIME RATIO

	AaSP-TP-FIPP / AaSP-FIPP (%)
30 *LRs*	26.1
45 *LRs*	26.5
60 *LRs*	25.6
75 *LRs*	24.8
90 *LRs*	25.4
105 *LRs*	27.2

(d)

RESULTS ON AVAILABILITY SATISFACTORY RATIO

Algorithms	Satisfactory Ratio(%)
PE-FIPP	93.3
AaSP-FIPP	96.1
AaSP-TP-FIPP	95.0

(e)

Fig. 2. (a) Spectrum utilization, (b) Working-to-backup ratio, (c) Distribution of protection schemes with Flex-TP-FIPP, (d) Running time ratio, (e) Service availability satisfactory ratio.

Next, we discuss how to conduct the topology partition in details. We first find all the unit cycles (UCs) in the topology, each of which contains the smallest number of nodes. For instance, for the US Backbone topology in Fig. 1(d), *Cycle* 1-2-4-2 is a UC. Then, we construct an auxiliary graph in which each UC is represented as a node and two nodes are connected if the two corresponding UCs share common link(s) (as shown in Fig. 1(e)). Finally, we conduct the topology partition in the auxiliary graph to distribute the UCs in each domain evenly and to cut as few links as possible. This is because we want to reduce the computation complexity for each domain and minimize the edge links. Fig. 1(e) and 1(d) show the topology partition result in the auxiliary graph and original topology, respectively. Note that, we also restrict the number of partitioned domains, since more domains would result in more optical-to-electrical-to-optical (O/E/O) conversions on the border nodes and hence increase the power consumption and cost.

In AaSP-TP-FIPP, we still first set up the working path for *LR* and check whether its availability requirement can be satisfied with the unprotected scheme. If not, starting from the source domain, we try to find an FIPP-*p*-cycle to protect the corresponding working path segment in each domain, for improving the request's availability. This procedure is repeated until the availability requirement is satisfied.

4. Simulation Results

We evaluate the proposed algorithms in the US Backbone topology, which is partitioned into three domains as shown in Fig. 1(d). The EON is assumed to accommodate 358 FS' (12.5 GHz) on each fiber link and the link availability is $\rho = 0.995$. The requests have their bandwidth requirements uniformly distributed within $[2,20]$ FS', availability requirements distributed within $[0.97, 0.9999]$, and minimum bandwidth requirements $\frac{B_m}{B}$ distributed within $[0.5, 0.9]$. We use the PE-FIPP algorithm developed in [6] as the benchmark for performance comparisons. The simulations are for static network planning, *i.e.*, all the requests are known and we arrange the working paths and FIPP-*p*-cycles with RSA to satisfy their bandwidth and availability requirements.

Fig. 2(a) shows the results on spectrum utilization. It can be seen that PE-FIPP uses the most spectra because it does not consider the availability requirements or bandwidth-squeezed restoration. AaSP-TP-FIPP achieves lower spectrum utilization than AaSP-FIPP, because with topology partition, it avoids to use relatively long FIPP-*p*-cycles and saves a lot of backup FS'. This can be verified with the results in Figs. 2(b) and 2(c), which indicate that AaSP-TP-FIPP provides the highest working-to-backup ratio among the algorithms and only 4% of the requests have FIPP-*p*-cycles in all the three domains in average. Note that, the topology partition can affect the algorithm's performance on availability satisfactory ratio, as the partial protection in certain domains is not as reliable as the end-to-end protection. This is the reason why in Fig. 2(e), the availability satisfactory ratio from AaSP-TP-FIPP is slightly lower than that from AaSP-FIPP. But both proposed algorithms achieve higher satisfactory ratio than PE-FIPP, which verifies the effectiveness of the proposed AaSP scheme. Finally, the results on running time ratio in Fig. 2(d) confirm that AaSP-TP-FIPP can reduce the time complexity effectively.

5. Conclusion

In this paper, we studied how to leverage FIPP-*p*-cycles to achieve spectrum-efficient AaSP in EONs. We incorporated bandwidth-squeezed restoration to design two novel AaSP schemes with and without topology partition. Simulation results showed that compared with the existing approach, our algorithms achieved ∼50% spectrum-saving.

References

[1] M. Liu, *et al.*, *J. Lightw. Technol.*, vol. 31, pp. 903–909, Mar. 2013.
[2] F. Ji, *et al.*, *J. Lightw. Technol.*, vol. 32, pp. 1190–1199, Mar. 2014.
[3] M. Clouqueur, *et al.*, *IEEE J. Sel. Areas Commun.*, vol. 20, pp. 810–821, Apr. 2002.
[4] Y. Sone, *et al.*, *J. Opt. Commun. Netw.*, vol. 3, pp. 223-233, Mar. 2012.
[5] A. Kodian, *et al.*, *J. Lightw. Technol.*, vol. 23, pp. 3241-3259, Oct. 2005.
[6] X. Chen, *et al.*, *J. Lightw. Technol.*, vol. 33, pp. 3719-3729, Sept. 2015.